J Mater Sci (2011) 46:77–89
DOI 10.1007/s10853-010-4819-3

Tow pullout behavior of polymer-coated Kevlar fabric

Anis Gawandi · Erik T. Thostenson · John W. Gilllespie Jr.

Received: 9 April 2010 / Accepted: 5 August 2010 / Published online: 21 August 2010

Abstract Tow pullout response of polymer-coated woven Kevlar fabric is investigated experimentally. Various material microstructures are created by applying heat and pressure to polymer-coated fabric to change polymer surface morphology. The pullout behavior is studied by conducting tow pullout tests using a pullout fixture. Single tow is pulled from the fabric loaded with tension in the direction transverse to that of pull. The tests are performed at various loading rates to investigate rate sensitivity of pullout load and energy. Load versus displacement data is obtained, from which the peak loads and pullout energies are computed. The results are compared with baseline neat fabric as well as baseline fabric with polymer coating. The results of the investigation show that for the Kevlar fabric under consideration, the neat fabric shows no loading rate dependence. On the other hand, the polymer-coated fabric shows loading rate dependence. Moreover, the heat-compressing of the fabric seems to have significant influence on tow pullout behavior. The results of pullout tests show that by simply compressing the fabric in the presence of heat may influence the interactions at tow cross-over regions to results in higher pullout energy.

A. Gawandi (✉) · E. T. Thostenson · J. W. Gilllespie Jr.
Center for Composite Materials, University of Delaware, Newark, DE 19716, USA
e-mail: gawandi@udel.edu

E. T. Thostenson
Department of Mechanical Engineering, University of Delaware, Newark, DE 19716, USA

J. W. Gilllespie Jr.
Department of Materials Science and Engineering, University of Delaware, Newark, DE 19716, USA

J. W. Gilllespie Jr.
Department of Civil and Environmental Engineering, University of Delaware, Newark, DE 19716, USA

Introduction

Woven fabrics like Kevlar®, Spectra®, and Zylon® are used in applications involving flexible structures subjected to dynamic loading. Due to the large energy that is transferred to the fabric in a dynamic loading event, high strength and high modulus fabrics like Kevlar are preferred in such applications. A woven fabric dissipates imparted energy through various damage mechanisms. Local tow failure at the point of impact, remote tow failure, and tow pullout are some of the energy dissipating failure mechanisms observed in the transverse loading of woven fabrics. Apart from the material properties and geometry, the velocity of the penetrator and its shape influence damage mechanisms and corresponding energy dissipations that may exhibit rate dependency.

Tow pullout is an important energy dissipating phenomenon wherein the tows that are impacted directly by the penetrator (principal tows) are pulled through the tow cross-over points. This mechanism is especially significant in the case of a penetrator with a blunt face impacting a fabric at non-penetrating velocities. For woven fabrics, tow pullout is influenced by the frictional properties at the tow cross-over points. Thus, altering the frictional properties at the cross-over points has a significant effect on the tow pullout behavior. Increasing the tow–tow friction at the cross-over points without premature yarn tensile failure is a plausible way to increase the pullout energy.

A class of tests reported in literature in conjunction with tow pullout behavior of woven fabrics is tow pullout tests. Briscoe and Motamedi [1] studied the effect of surface

friction characteristics of aramid fabrics with respect to their static deformation and dynamic performance. Various fabric weaves were studied with different levels of yarn–yarn friction achieved with addition or removal of surface lubricants. It was found that fabrics with high friction dissipated larger amount of energy relative to the fabrics with lower friction for both quasi-static and dynamic deformation processes. Bazenov [2] studied the pullout zones created by dynamic impact of laminates comprising several aramid fabric layers. He performed yarn pullout tests on plain-weave aramid fabric with varying yarn–yarn friction levels. Also, effect of water on pullout behavior was tested by immersing the fabric in water before testing. It was concluded that energy transferred to fabric increases with volume of pullout zone. Also, water reduced the penetration resistance of laminates owing to reduction of the width of pullout zone.

Shockey et al. [3] performed pullout tests on single yarn pulled from a fabric layer while the fabric is preloaded in tension in the direction transverse to that of the yarn being pulled out. Force–displacement data was recorded. The tests were performed on Zylon (30 × 30 and 40 × 40), Kevlar (32 × 32), and Spectra (32 × 32) fabrics for various pullout rates. Both warp and fill yarns were pulled from the fabric. The results showed significant effect of pullout rate for Zylon, a smaller effect on Spectra, and a negligible effect for Kevlar. Kirkwood et al. [4] performed yarn pullout tests on Kevlar KM2 600 denier fabric preloaded in tension in the transverse direction. Effects of fabric length, number of yarns pulled, arrangement of yarns, and transverse tension on the force–displacement curves were studied. A semi-empirical model was presented for predicting the yarn pullout energy as a function of pull-out distance. The model was observed to replicate the experimental data with high degree of accuracy. The energy of yarn pullout from a fabric was found to depend on length of sample, transverse fabric tension, number of yarns pulled at once, and distance the yarn was pulled.

In addition to some of the empirical studies discussed above, many researchers have used numerical approach to gain an insight into the fabric behavior under a dynamic loading event [5–8]. Majority of these studies involve numerical simulations using linear elastic properties and do not model individual tow–tow interactions. Shockey et al. [3, 9] analyzed plain-weave Zylon fabric assuming frictionless interactions. Duan et al. [10] modeled single-layer woven fabric considering tow–tow interactions and reported that frictional interactions at tow cross-over points play a significant role in dynamic energy absorption. Zeng et al. [11] investigated the influence of inter-yarn friction on the ballistic performance of woven fabric. Frictional sliding between yarns was implemented in the computational model. Parametric studies showed that ballistic response of the fabric was very sensitive to yarn–yarn friction when the friction coefficient was low, but insensitive beyond a certain level. Pan and Yoon [12] modified the analytical model developed for nonwoven structures to describe yarn pullout process. The theory was able to predict the relationship between maximum pullout load and embedded yarn length in the fabric. Experimental work was performed and shown to verify the analytical predictions. Valizadeh et al. [13] developed an analytical model of yarn pullout which predicted the internal mechanical parameters of the fabric using a force balance approach. Some of these parameters were yarn-to-yarn friction coefficient, normal load at crossovers, lateral forces, lateral strain, weave angle variations, and pullout force. These parameters were predicted on the basis of fabric deformation data collected experimentally. The study showed that force balance model predictions correlated with the experimental yarn pullout data. Finally, Kalman et al. [14] investigated the penetration behavior of Kevlar fabric intercalated with dry particles and shear thickening fluids. Tow pullout tests were performed to evaluate the influence of these fabric treatments on the pullout behavior. Results indicated that presence of particles in the fabric enhanced pullout energy relative to neat fabric.

Most of the research efforts described above are focused on woven neat fabric or fabric layers of various materials. Another class of woven fabric materials is the one in which the fabric is coated with a small amount of polymer. Of particular interest as a coating material are the ethylene copolymers like ethylene/methyl acrylate copolymer. In some cases, the reason for coating the fabric with polymer is to reduce the transverse deflection of the fabric in the case of a dynamic loading event. At the same time, the frictional properties at the cross-over points of the fabric can be influenced in the presence of a coating material in the cross-over regions of the fabric. The tow–tow interactions can be altered to an extent that the gross fabric pullout energy is different from that for a corresponding neat fabric. The question therefore arises as to how the polymer morphology on the surface of a plain-weave fabric alters the tow pullout response. Especially, the influence of processing temperature and pressure on the tow pullout behavior needs to be investigated in light of the presence of a polymer coating on the tow surface. Previous studies have reported the dependence of mechanical properties of ethylene copolymers on polymer morphology. Ma et al. [15] investigated the relationship between the morphology and the mechanical properties of EMMA films as a function of temperature. X-ray diffraction measurements revealed that crystallinity in the polymer decreased as temperature increased. The results of the investigation showed that the mechanical properties like modulus and yield strength of the EMMA polymer decreased with increasing temperature. Thus, an understanding of this aspect can potentially help to identify a

particular morphology that maximizes the tow pullout energy without causing premature tow tensile failure.

In this study, experimental investigation of tow pullout behavior of plain-weave Kevlar KM2 fabric coated with a polymer is undertaken. Polymer morphology on the fabric surface is altered by applying temperature and pressure. Tow pullout tests are performed on a single layer of Kevlar fabric subjected to transverse tension. Load–displacement curves for a single tow pullout are generated for various material configurations at various loading rates and transverse tension. Pullout energies are subsequently computed. The results obtained are compared with those for the neat fabric without any coating material. The influence of polymer surface morphology on the tow pullout behavior is discussed.

Materials

Baseline neat Kevlar fabric

The Kevlar fabric used is plain-weave Kevlar KM2 from DuPont®. The measured linear density of the fabric is 850 denier. The fabric has approximately 10.5 yarns per cm (warp and fill). The uncoated version of the fabric has a measured areal density of 211 g/m^2. The measured crimp frequencies for the fabric in the warp and fill directions are 14 and 13 per inch, respectively. Figure 1 shows the scanning electron microscopy (SEM) image of the baseline neat fabric.

Baseline polymer-coated fabric

The coated version of the Kevlar KM2 fabric has a coating of Vamac® which is an ethylene/methyl acrylate copolymer [16]. The copolymer has a zero shear rate melt viscosity in the range of 2×10^6 to 10^{13} poise at 20 °C [17]. It has a glass transition temperature (T_g) of −30 °C [17]. The tensile modulus at 100% strain for Vamac compounds range from 5 to 6 MPa, whereas the tensile strength ranges from approximately 14–16 MPa [16]. The coating is applied by the fabric manufacturer [17]. Figure 2a and b shows SEM images of both sides of the as-received fabric. A resin-rich side to the fabric, possibly due to the coating process, is clearly visible.

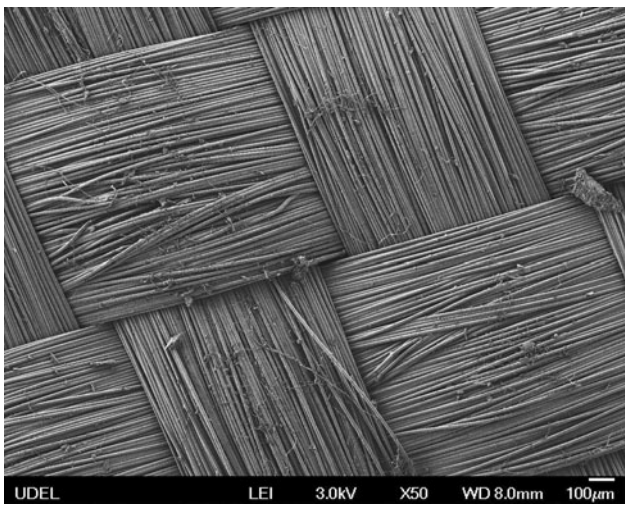

Fig. 1 SEM images of baseline neat Kevlar KM2 fabric

Polymer-coated fabric with modification to polymer surface morphology

The surface morphology of the polymer-coated fabric is altered by compressing the fabric at various temperatures. Harkare and Gillespie [18] quantified the effect of pressure, temperature, and time on the spreading and tow impregnation of thermoplastics into fabrics that explains the changes of surface morphology observed in this study. Here we hold the compaction time and pressure constant and vary the temperature to control the morphology. The fabric layer is heat-compressed at the temperatures of 75, 100, and 150 °C at an approximately constant pressure of 0.86 MPa (125 psi) for 15 min. The fabric compression under temperature results in lateral spreading of the polymer on the surface of the fabric followed by transverse impregnation of the fiber bundles. Increased temperatures reduce the polymer viscosity and alter the timescale of the spreading and transverse impregnation process and results in different polymer morphologies on the fabric surface. After the application of temperature and pressure, scanning electron microscopy is used to examine the change in surface morphology.

Figure 3 shows an SEM image of the resin-rich side of the fabric compressed at 75 °C. The elevated temperature compression at this temperature drives the polymer on the resin-rich front face towards the interlacing regions and results in the concentration of resin. Unlike the fabric compression at 75 °C, where the polymer has been concentrated in the interlacing regions (Fig. 4a), heat-compressing at 100 and 150 °C results primarily in transverse infiltration into the fiber bundles (Fig. 4b). SEM images of fabric processed at 150 °C shows a similar infiltrated morphology.

These differences in polymer surface morphology may have a significant influence on tow–tow interactions as these interactions can occur from mechanical interlocking of polymer between tows or the healing of polymers across the tow interface during compression molding [19]. The SEM micrographs in Fig. 5 show the fiber surfaces of bundles extracted from the fabric near the crossover point in the interlacing region of the baseline coated fabric and the fabric processed at 75 °C. In the baseline coated fabric

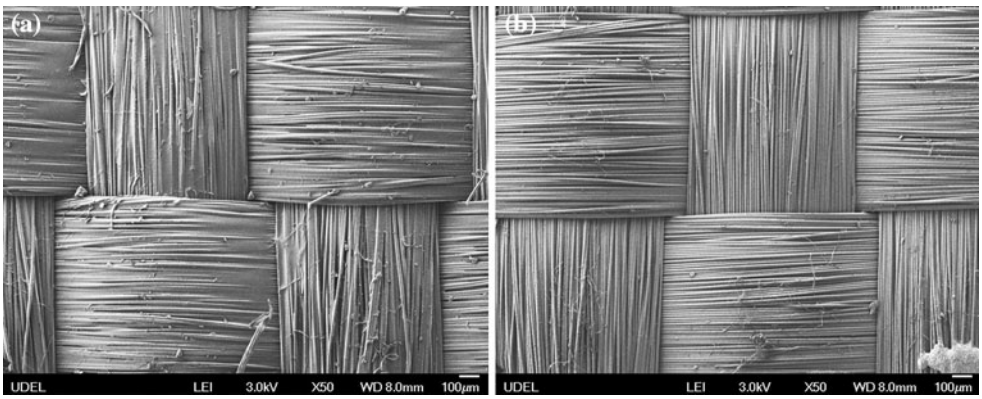

Fig. 2 SEM images of baseline coated Kevlar KM2 fabric showing **a** a polymer rich surface and **b** a surface with little polymer coating

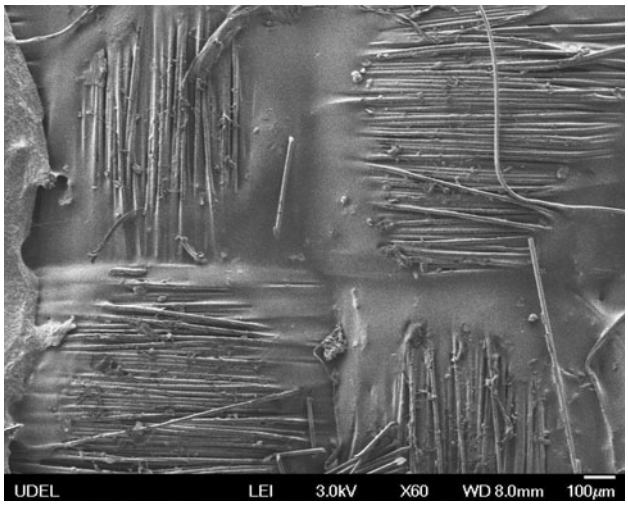

Fig. 3 SEM micrograph showing the polymer morphology on the resin-rich surface resulting from fabric compression at 75 °C. The fabric compression results in polymer concentration in fiber bundle interlacing regions

there is relatively little polymer observed on the fiber surfaces. However, in the fabric processed at 75 °C there is a substantial amount of polymer that has been forced into the regions between the fiber bundles. The pattern of the polymer clearly shows an impression left by the removed fiber bundle that was previously on top of this area, indicating enhanced tow–tow interactions.

Based on the observations from the scanning electron microscopy, the modified fabrics are classified as:

1. Modified coated Kevlar KM2 processed at 75 °C (MP-75).
2. Modified coated Kevlar KM2 processed at 100 °C (MP-100).
3. Modified coated Kevlar KM2 processed at 150 °C (MP-150).

Experimental setup

Figure 6a shows the schematic of the tow pullout test. All tests are performed by pulling a single tow from a single layer of fabric while preloading the fabric in tension in the transverse direction. A fabric layer approximately 190 mm in size is used for the test. Yarns transverse to the direction of the pullout are manually removed to free up

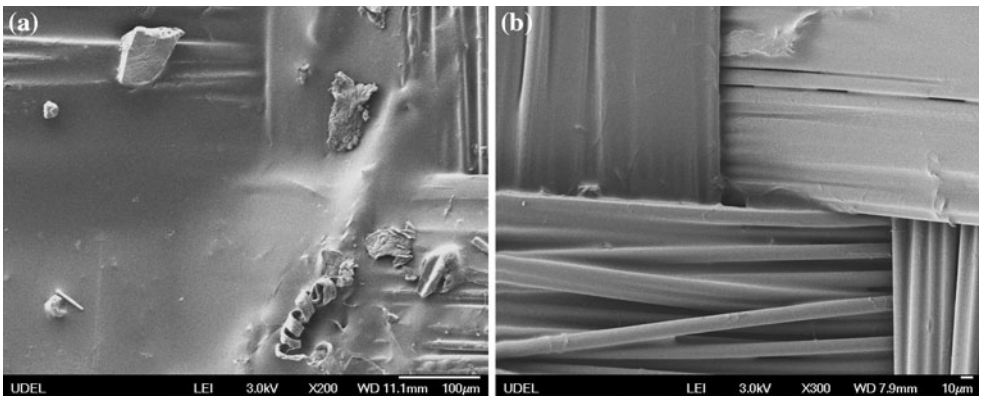

Fig. 4 SEM image of the fabric specimen compressed at **a** 75 °C and **b** 100 °C, showing increased transverse infiltration into the fiber bundles at higher temperature

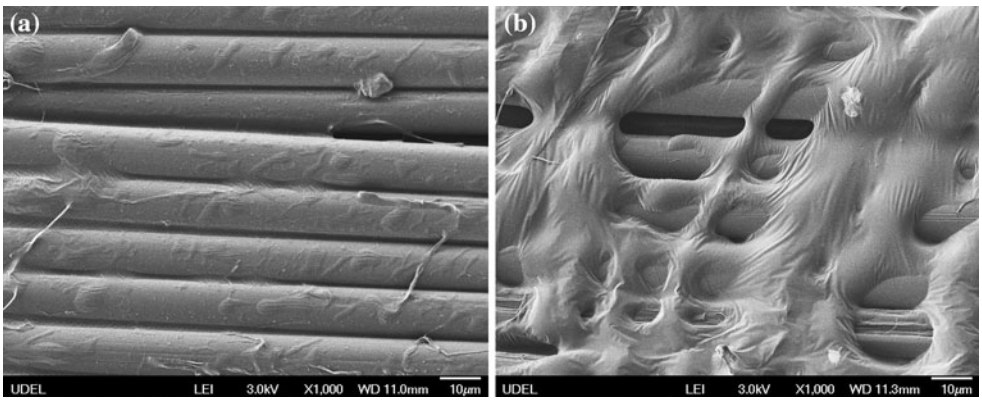

Fig. 5 Images of extracted fibers near the crossover point in **a** baseline coated fabric and **b** fabric processed at 75 °C

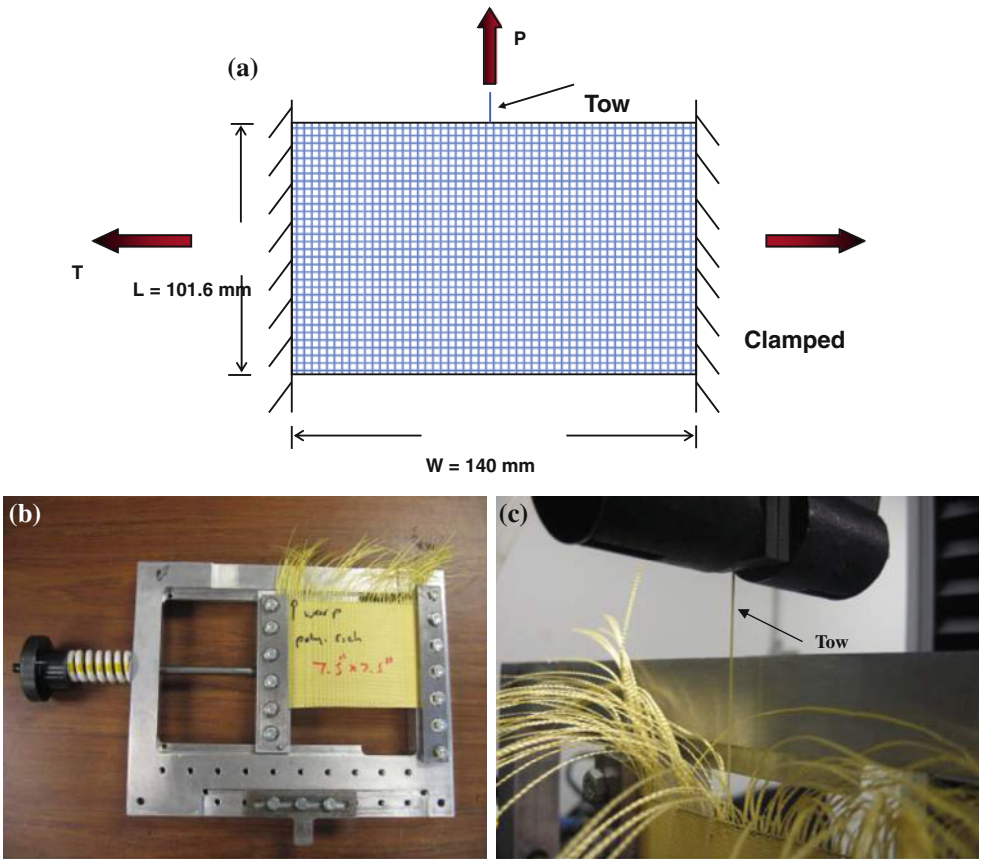

Fig. 6 **a** Schematic of tow pullout test, **b** tow pullout fixture, and **c** experimental setup

approximately 88 mm length of yarns to grip in the machine. The remaining approximately 102 mm length of the fabric is clamped in the direction of the pull. This length (L, see Fig. 6a) is kept constant for all experiments. With this length, approximately 108 cross-over points are available for the tow to pull through. Shockey et al. [3] found that multiple yarns can be pulled from a single fabric without altering the pullout behavior if at least two yarns are in between the successive yarns pulled. This observation is first verified prior to testing and although leaving two yarns in between seems to be sufficient, it is decided to leave at least three yarns between the successive tows being pulled. All tests are conducted using an Instron 5567 machine with a 500 N (100 lb) load cell.

Figure 6b shows the fixture used for the tow pullout tests. The fixture is adapted from Shockey et al. [3] and is similar to the one used by Kirkwood et al. [4]. It allows for a fabric specimen to be clamped on opposite edges using screws. The fabric edge to be clamped is wrapped over a steel rod that fits in a trench on the fixture. A top plate is

then placed firmly and tightened with screws. Approximately 25 mm of fabric length at each end is provided for this wrapping and clamping mechanism. The fabric specimens are cut such that approximately 140 mm length of fabric remained between the two clamped edges. This length is also kept constant for all experiments. The fixture uses a spring-mounted sliding edge as one of the two supports to apply transverse tension on the fabric specimen. Precise value of the transverse tension is set by compressing the spring using a fine thread nut. Knowing the spring constant, the nut is moved through a predetermined number of threads to set a given tension value. The fixture is mounted in the Instron machine at its bottom using 90 psi pneumatic grips. The upper pneumatic grip is used to grab onto a single tow to be pulled out of the fabric. Figure 6c shows the actual test set up for the tests.

The pullout tests are performed under displacement control at three different displacement rates of 5.08, 50.8, and 508 mm/min. Also three different transverse tension values of 2.45, 4.9, and 9.8 N/mm are used. Considering the variation of crimping in the warp and weft directions of the fabric, pullout tests are performed in both warp and weft directions. Five tests are conducted for each configuration. Load versus displacement data is collected from the machine for each test for data reduction. A very good repeatability is seen in the tests for all different materials considered. Table 1 shows the average values of peak loads and pullout energies discussed in the following sections based on five replicas tested at each configuration. The table also shows corresponding standard deviations and coefficients of variation, which clearly shows a very good repeatability of the experimental data for the various configurations tested. As shown by the collected load–displacement data is used to characterize the pullout behavior and compute pullout energies for various cases considered. The results from the tests are discussed in detail in the following section.

Results and discussion

Influence of loading rate

During the pullout tests on baseline neat Kevlar fabric, no visual change is observed in rest of the fabric as the tow is being pulled at the various loading rates Fig. 7 shows the load–displacement plot from a set of pullout tests in the warp direction of the neat Kevlar fabric for a transverse tension of 250 N. The complete tow pullout process shown in the figure comprises two parts. In the beginning, as the load is applied on the tow, the tow starts uncrimping. This process is represented by the initial linear portion of the

Table 1 Peak loads and normalized pullout energies for various configurations along with corresponding standard deviations

Material	Load rate (mm/min)	P_{max} (N)	Standard deviation	Coefficient of variation	EP/AD (J/N/m^2)	Standard deviation	Coefficient of variation
Neat Kevlar—warp	5.08	22.64	0.55	2.43	0.362	0.005	1.38
	50.8	24.06	0.4	1.66	0.377	0.008	2.12
	508	22.73	1.486	6.54	0.386	0.02	5.18
Neat Kevlar—fill	5.08	12.65	0.36	2.84	0.226	0.008	3.54
	50.8	12.47	0.292	2.34	0.222	0.008	3.60
	508	13.19	0.426	3.23	0.262	0.009	3.44
Coated Kevlar—base warp	5.08	29.35	0.268	0.91	0.484	0.013	2.69
	50.8	39.47	1.243	3.15	0.681	0.004	0.59
	508	54.5	1.852	3.40	0.991	0.034	3.43
Coated Kevlar—base fill	5.08	28.33	0.589	2.08	0.484	0.013	2.69
	50.8	30.3	1.833	6.05	0.604	0.043	7.12
	508	44.35	0.978	2.21	0.9	0.028	3.11
MP-75 warp	5.08	34.61	0.451	1.30	0.677	0.013	1.92
	50.8	53.79	2.642	4.91	1.058	0.042	3.97
	508	79.09	2.453	3.10	1.467	0.06	4.09
MP-100 warp	5.08	33.69	0.379	1.12	0.458	0.007	1.53
	50.8	48.15	1.332	2.77	0.754	0.035	4.64
	508	69.86	0.297	0.43	1.204	0.035	2.91
MP-150 warp	5.08	29.26	2.01	6.87	0.363	0.03	8.26
	50.8	43.48	0.154	0.35	0.538	0.003	0.56
	508	59.5	1.33	2.24	0.773	0.016	2.07

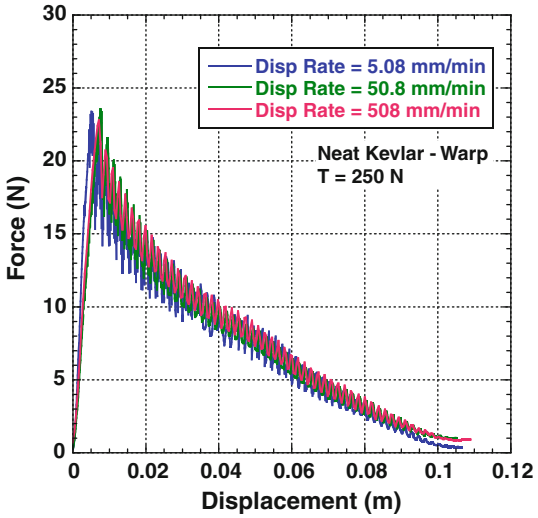

Fig. 7 Load–displacement curves for the baseline neat fabric in the warp direction

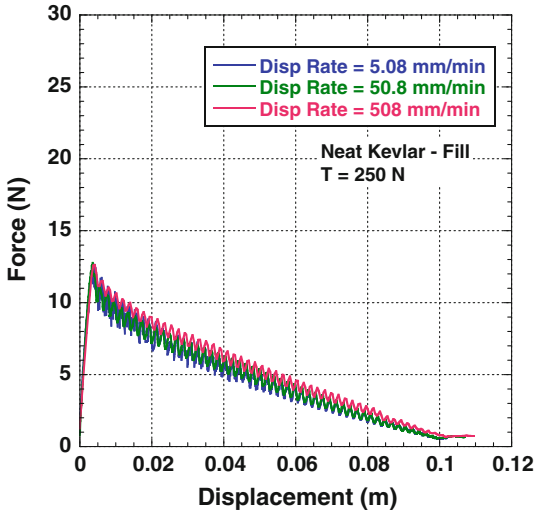

Fig. 8 Load–displacement curves for the baseline neat fabric in the fill direction

force–displacement curve. One can visually notice the change in the appearance of the tow during the uncrimping process. During the tow uncrimping, the tow being pulled experiences static friction at the cross-over points. Once the peak load is reached, the tow uncrimping stops and the tow starts to move. This is called tow translation and is represented on the force–displacement curve in the post-peak region. Obviously, during its translation through the fabric, the tow experiences kinetic friction at the cross-over points. Tow translation is always preceded by tow uncrimping. The translation part of the curve is characterized by the oscillations in the post-peak part of the curve. These oscillations result from the transition of the yarn through the cross-over points. As the tow translates through the fabric, it encounters less and less number of cross-over points which results in gradual drop in the load until the tow is completely pulled out of the fabric. At this point the load drops to zero.

As Fig. 7 shows, the baseline fabric without any coating shows no loading rate dependence. The curves for various loading rates almost fall on top of each other. Figure 8 shows the load–displacement plot for the fill direction of the baseline neat fabric. Although a similar trend is seen in the fill direction of the baseline neat fabric in terms of rate dependence, the peak loads are approximately 80% smaller than those in the warp direction. When observed under microscope, the fabric under consideration clearly shows a larger crimp in the warp direction which explains the difference observed in the tow pullout behavior in the two directions.

Unlike the neat fabric, all coated fabrics (baseline and modified) show a slight elastic deformation in the pullout direction as shown in Fig. 9a and b. This deformation can be seen during most of the pullout process with fabric gradually reverting to original position as the tow is pulled out of the fabric. Figure 9a shows the initial part of the pullout process before the peak load is reached. During this process successive cross-over regions yield progressively. This is clearly showed by the changed appearance of approximately top half of the tow in the fabric. Note that the bottom half of the tow segment in the fabric shows no visual change at this point. It is also observed that at this point, a point on the tow at the top has clearly shifted up confirming the uncrimping of the tow. During this progressive yielding, the tow uncrimps and peak pullout force is reached as the tow uncrimps fully. Upon uncrimping, the tow starts to move through the fabric. This stage is shown in Fig. 9b. The black streak at the bottom of the tow shows the cross-over points the tow has transitioned through.

All Vamac-coated fabrics clearly show loading rate dependent tow pullout behavior as shown by Figs. 10, 11, 12, and 13. Figure 10 shows the load–displacement curves for the baseline Vamac-coated fabric. The curves for different loading rates are now well separated from one another unlike the neat fabric. The loading rate dependence can be observed for initial linear parts of the load–displacement curves up to the peak load and also the post-peak part. The successive increasing loading rate curves completely envelope the previous curves. The peak load now increases with the increasing displacement rate. Also, the linear portion of the curve shows stiffening effect as the displacement rate is increased. A comparison shows that the peak load at the largest displacement rate of 508 mm/min is almost 45% larger than the corresponding baseline coated fabric case. The peak loads at the other displacement rates are also significantly greater than the corresponding neat fabric case. Also, the greater the loading rate, the more subdued these oscillations are. Even after the

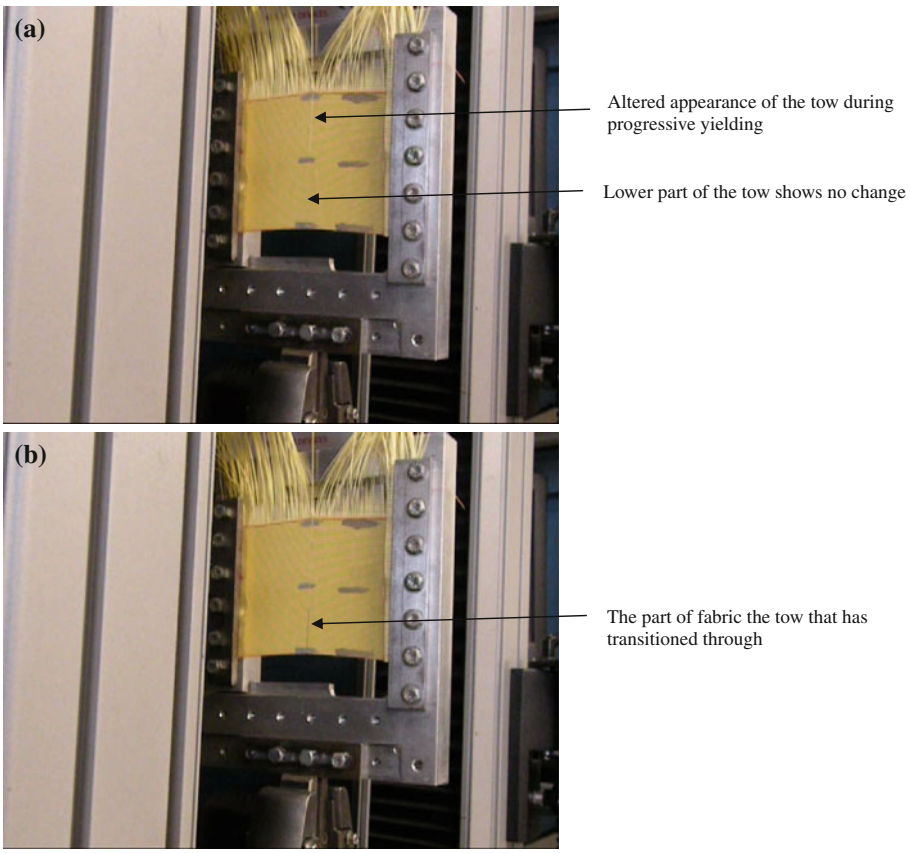

Fig. 9 **a** Progressive yielding at the cross-over points for coated fabric during the initial part of the pullout before peak load is reached. **b** Tow transition through the cross-over points in the fabric during the post-peak stage of the loading

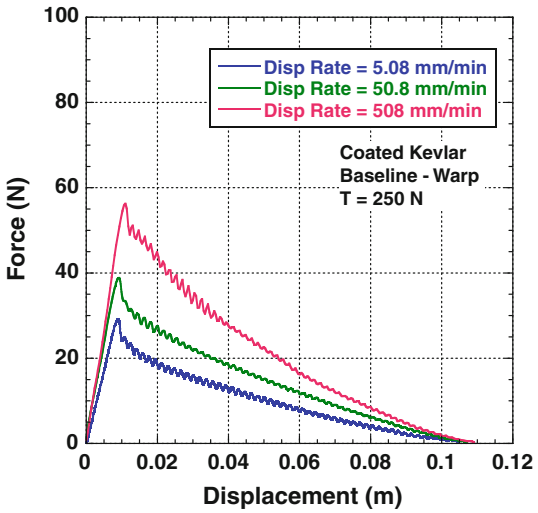

Fig. 10 Load–displacement curves for the baseline polymer-coated fabric in the warp direction

peak force is reached, the oscillating force corresponding to tow translation through the fabric does not return to the post-peak values obtained for corresponding baseline neat fabric and remains larger than the baseline neat fabric. The presence of polymer on the fabric surface, especially in the cross-over regions seems to introduce the rate dependent tow pullout behavior in the fabrics with polymer coating. The polymer at the cross-over points seems to enhance both static and kinetic frictional effects as evident from the force–displacement curves.

The pullout tests on tows from the fabrics with modified polymer morphology (MP-75, MP-100, and MP-150) reveal that the tow pullout behavior is sensitive to the altered polymer morphology. All modified fabrics show greater peak loads relative to the baseline coated fabric. Figure 11 shows the test data for the MP-75 fabric (polymer concentrated in undulations). The enhancement in the peak loads over the baseline Vamac-coated fabric can be clearly seen. Also, the oscillations in the post-peak region of the curve seem to be substantially subdued. The MP-75 fabric specimen gives the largest peak load among all fabrics considered in this study. The force–displacement curves for the modified fabrics MP-100 and MP-150 are shown in Figs. 12 and 13. The tow pullout tests for modified fabrics MP-100 and MP-150 show an increase in peak loads relative to the baseline coated fabric. However, the peak loads are smaller compared to the other modified morphology (MP-75). The load–displacement behavior for these two fabrics appears similar to that of the baseline coated fabric with the exception of increased peak loads. Figure 14 summarizes the loading rate dependent behavior of various fabrics tested at the transverse tension value of 250 N. Increase in the peak load is showed as a percent

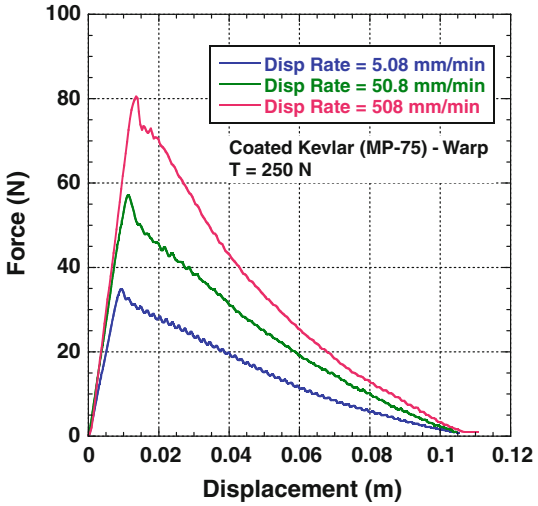

Fig. 11 Load–displacement curves for the modified fabric MP-75 fabric in the warp direction

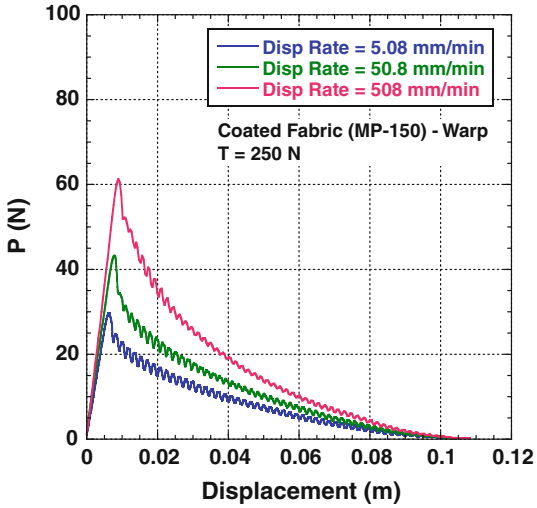

Fig. 13 Load–displacement curves for the modified fabric MP-150 fabric in the warp direction

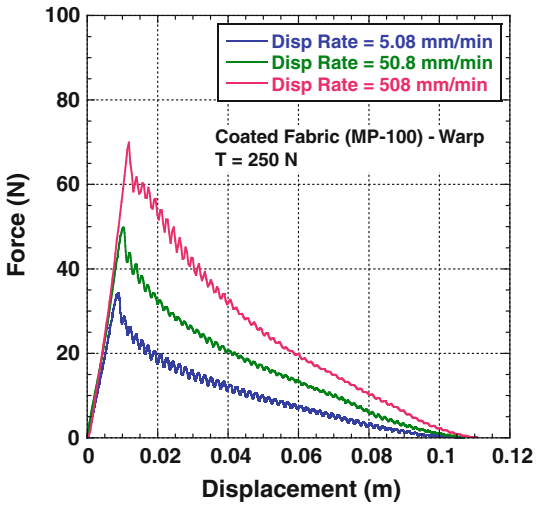

Fig. 12 Load–displacement curves for the modified fabric MP-100 fabric in the warp direction

increase over the peak load for the baseline neat fabric in the fill direction (smallest peak loads of all). The rate dependence of Vamac-coated fabrics and the greater peak loads for modified fabrics are evident from this summary.

As mentioned above, the fabrics with modified polymer morphology show increased peak loads. Note that the fabric with the largest peak load denoted as MP-75 seems to have polymer concentrated in the undulation areas as discussed previously (Fig. 4a, b). The fabric MP-100 shows the second largest peak load increase among the various fabrics considered. On the other hand, in the case of the other modified fabrics (MP-100 and MP-150), the compression of the fabric under elevated temperature resulted in flow of polymer away from cross-over regions due to increased viscosity (Fig. 5). As a result, the peak load increase for these cases is smaller than the MP-75 fabric. Additionally, the altered polymer morphology may have also contributed to the strain rate sensitivity seen in the polymer-coated fabrics.

From the above discussion, it seems that for the Vamac-coated fabric, there may be a simple modification that will result in a modified polymer morphology that will enhance the pullout response of the fabric. The peak loads in the pullout tests are important because increasing the peak load will increase the total pullout energy if other parameters remain relatively unchanged. On the other hand, the tow tensile strength is the upper limit for the likely enhancement in the peak load. If the tensile strength is exceeded, there will be tow tensile failure before the pullout process is completed. An evaluation of peak loads in this study shows that the peak loads are still significantly smaller than tow tensile strength. For an estimated tensile failure load of 125 N [15], the largest peak load obtained (for the MP-75 case at the displacement rate of 508 mm/min) is still approximately 65% of the tow tensile strength. For the baseline coated fabric case, the largest peak load obtained is approximately 45% of the tow tensile strength. Thus, for the pullout length considered in this study, an improvement in the peak loads is clearly achieved by compressing the fabric at elevated temperatures without approaching the tensile strength of the tow. Indeed there may be a temperature–pressure condition that will further drive the peak loads up without causing tensile failure of the tow.

Pullout energy

The area under the force–displacement pullout curve gives the total pullout energy for the single tow pullout. The total

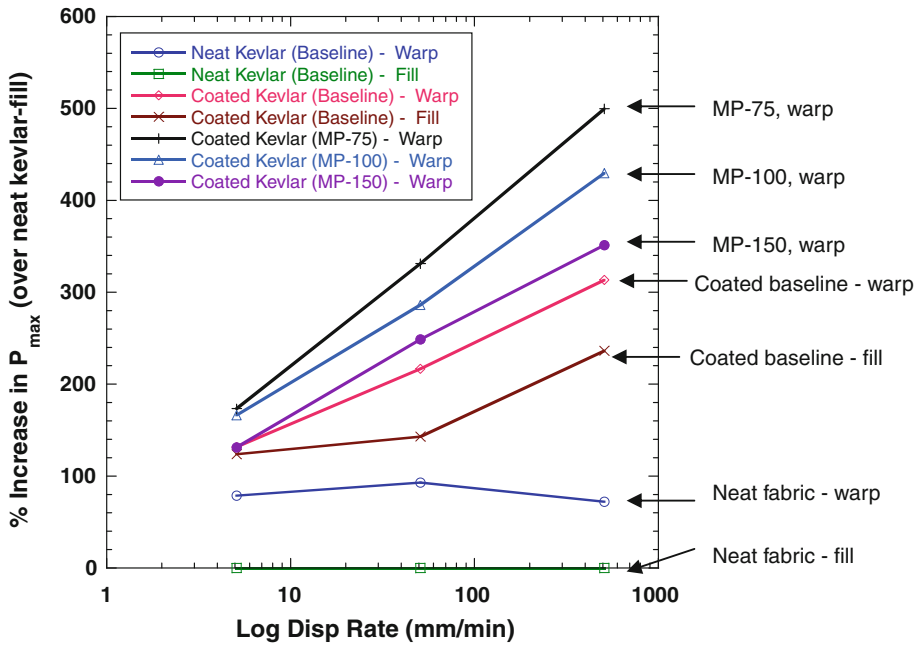

Fig. 14 Increase in peak load as a function of loading rate for various fabrics in pullout tests

pullout energy is composed of the tow uncrimping and tow translation parts [4]. Therefore:

$$E_{\mathrm{P}} = E_{\mathrm{U}} + E_{\mathrm{TR}} \tag{1}$$

The tow uncrimping energy is given by the area under the linear part of the load–displacement curve up to the peak load. Once the peak load is reached, the tow uncrimping stops and the tow starts to move giving rise to the post-peak region in the curve. The tow translation energy corresponding to this event is given by the area under the translation part of the load–displacement curve. The total pullout energy is obtained by adding these contributions.

Figure 15 shows the total tow pullout energy as a function of displacement rate for various fabrics for warp direction pullout. The pullout energy presented in the figure has been normalized with respect to the areal density of the corresponding fabric. With the exception of the baseline neat fabric, the total pullout energy increases with increased loading rate. The largest pullout energy corresponds to the fabric MP-75 which has modified polymer morphology with polymer concentration in the interlacing regions. This material configuration also showed the largest peak loads of all materials. On the other hand, the pullout energy for the fabric MP-100 is smaller than that for the fabric MP-75 at all loading rates, although it is greater that for the baseline Vamac-coated fabric. The other modified fabric MP-150 shows pullout energy that is smaller than both MP-100 and baseline Vamac-coated fabric. A closer examination of the load–displacement response of this fabric reveals that the fabric has a smaller uncrimping and translation energy components compared to the baseline coated fabric in spite of larger peak loads. Also, a closer examination of force–displacement plots in Figs. 7, 8, 10, 11, 12, and 13 reveals that the major contribution to the total pullout energy comes from the post-peak tow translation part of the load–displacement curve. This contribution ranges from 88 to 95% of the total pullout energy for various fabrics considered in this study. This range seems to be constant at various loading rates used in the experiments.

From Fig. 15 it is clear that modification in the polymer surface morphology through heat-compression results in enhanced pullout energy for the polymer-coated Kevlar fabric. The enhanced pullout energy means an increased contribution from tow pullout mechanism to the total absorbed energy in the event of dynamic impact of a projectile on the fabric. Therefore, a simple compression of polymer-coated fabric at an optimum temperature and pressure setting has a potential of enabling this improvement in the fabric performance.

SEM analysis of tows after pullout

As a tow is pulled out of the fabric, the cross-over regions along the tow experience frictional contact from the transverse tows. The cross-over points at the top of the tow transition through smaller number of cross-over regions compared to those near the bottom. In this study, there are approximately 98 cross-over regions in the tows pulled from the fabric specimens. Thus, the part of tow at the bottom of the fabric specimen goes through 98 cross-over locations before it is completely pulled out of the fabric. In order to investigate the effect of this transition on the tow surface and possibly on the tow pullout force during

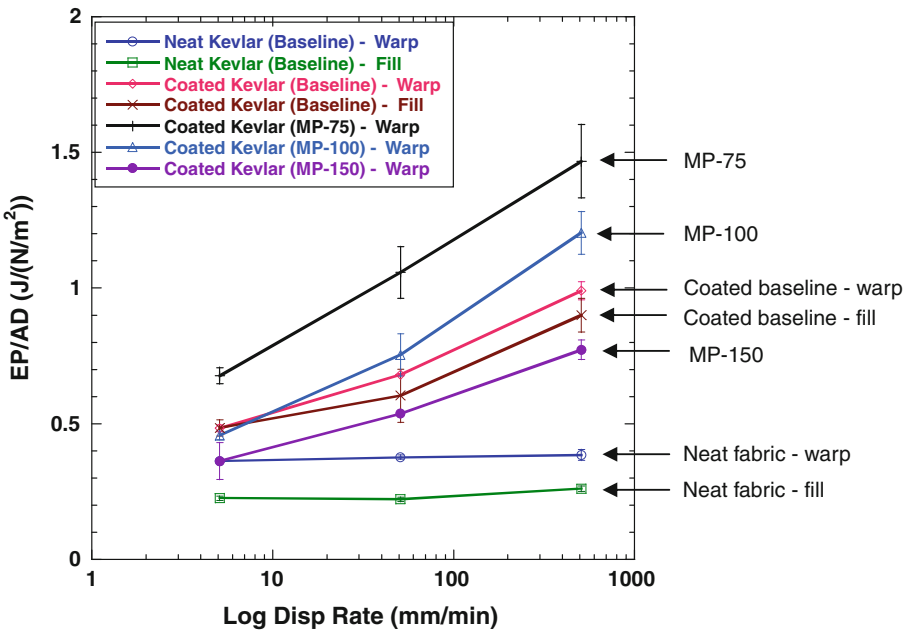

Fig. 15 Pullout energies for various fabrics normalized by the respective aerial densities

the post-peak part of the loading, the pulled polymer-coated tows are analyzed using the scanning electron microscopy imaging. The SEM analysis is conducted on tows pulled at the smallest (5.08 mm/min) and largest (508 mm/min) loading rates employed. Figures 16, 17, and 18 show the results of the SEM analyses.

Figure 16a and b shows the tow surfaces before pullout for MP-100 and MP-75 modified fabrics. Note that the baseline Vamac-coated, MP-100, and MP-150 fabrics showed transverse infiltration into fiber bundles, whereas the fabric MP-75 showed polymer concentration at the interlacing regions. Figure 17a and b shows the top and bottom cross-over regions of the tow extracted from the polymer-coated fabric MP-100, respectively, from the pullout test at the smallest loading rate. The fabric has a modified polymer morphology resulting from heat-compression treatment. As the figures show, there is little difference between the two in terms of the change in the surface texture due to pullout. The tow surface appears very similar to the surface before the pullout. On the other hand, the tow pulled at the largest loading rate shows change in surface texture as shown in Fig. 17c and d. Especially, the bottom part of the tow which travels through maximum number of contact regions shows less ductile type of polymer fracture on the surface as shown in Fig. 17d. The top part also shows somewhat similar polymer fracture with less ductility apparent. The other configurations namely, baseline polymer-coated, modified fabric MP-150, and MP-75 also show post-pullout surface textures similar to those seen in the MP-100 material.

Figure 18a and b shows high magnification images of the tow surface at the bottom for the MP-100 fabric tested at 508 mm/min. The brittle fracture of the polymer can be clearly seen in the images. The images show clumps of polymer debonded from the fiber surfaces in the tow. The polymer–fiber interface failure seems to be a mixture of the adhesive failure at the fiber–polymer interface and cohesive failure of the polymer itself.

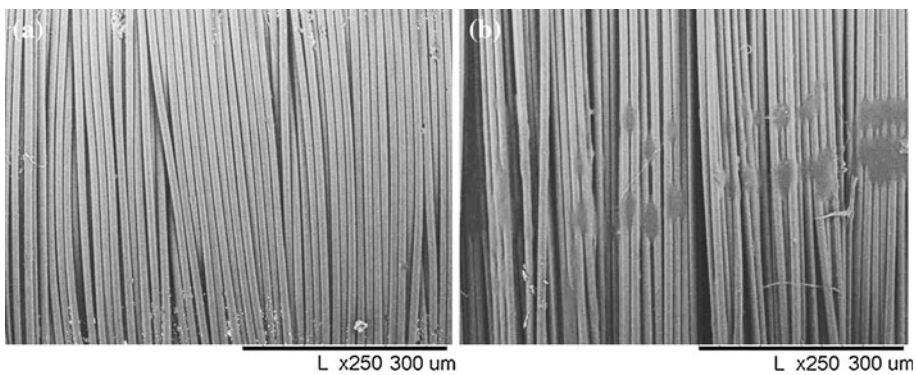

Fig. 16 Tow surface at cross-over points before pullout for **a** fabric PTI-10 and **b** fabric MP-75

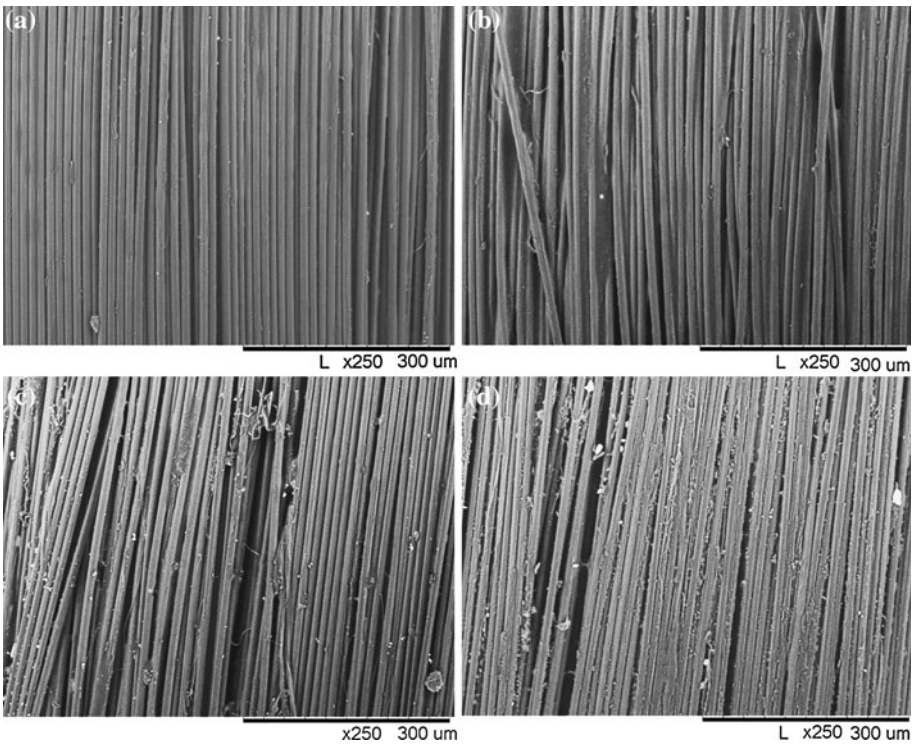

Fig. 17 Tow surface at cross-over points after pullout for MP-100 fabric **a** top of the tow at 5.08 mm/min, **b** bottom of the tow at 5.08 mm/min, **c** top of the tow at 508 mm/min, and **d** bottom of the tow at 508 mm/min

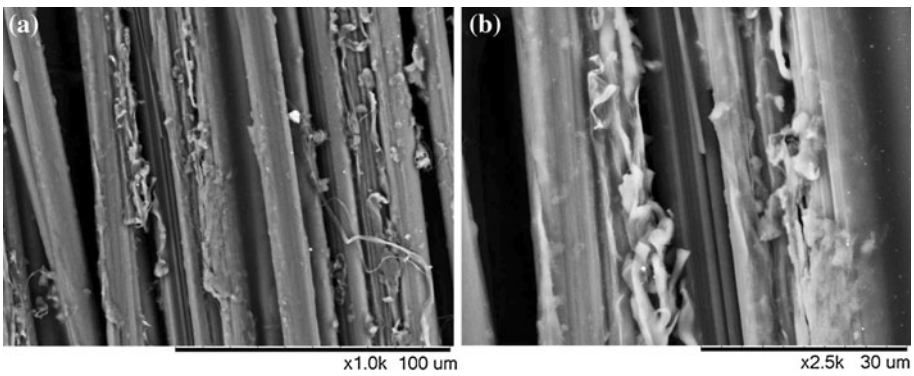

Fig. 18 High magnification images of tow surface at cross-over points after pullout for MP-100 fabric showing the nature of fracture of polymer. The images show the bottom of the tow tested at 508 mm/min

Conclusions

Tow pullout tests are performed on various Kevlar fabrics with and without polymer coating on the fabric surface. Moreover, the polymer-coated fabrics are modified to alter polymer surface morphology by compressing the fabric under various temperatures and constant pressure. Pullout tests are performed on these fabrics at various loading rates. Single tow is pulled out from fabric specimens loaded transversely using a pullout fixture. Force versus displacement data is acquired to compute pullout energy. The peak loads and total pullout energies from this data are compared to baseline neat fabric and baseline coated fabrics to evaluate the improvements due to fabric modification.

The results of the pullout tests show that modification to the polymer morphology on the fabric surface significantly influences the pullout behavior in the case of polymer-coated fabrics. All polymer-coated fabrics show a loading rate dependent pullout behavior, wherein the progressive yielding failure takes place at the cross-over points of the tow. Two out of the three modified fabrics show enhancement in peak loads relative to the baseline fabrics. Also, these modified fabrics give the largest pullout energies among all configurations considered. Especially, the fabric with polymer concentration in the undulation areas shows the best enhancement in pullout energy. The SEM analysis of pulled tows from polymer-coated fabrics shows no significant variation in the tow surface texture at small loading rate. However, moderate to significant change in the tow surface texture is observed at the largest loading rate. Finally, a simple fabric compression in the presence of temperature may be used to enhance the fabric energy absorbed by tow

pullout mechanism provided the energy absorbed from other damage mechanisms remains relatively unchanged. This may be a significant considering that the presence of polymer coating on the fabric results in decreased fabric performance in a dynamic loading event.

Acknowledgement This work was supported by E. I. du Pont de Nemours and Company, Wilmington, DE.

References

1. Briscoe BJ, Motamedi F (1992) Wear 158:229
2. Bazenov S (1997) J Mater Sci 32:4167. doi:10.1023/A:1018674528993
3. Shocky DA, Erlich DC, Simons JW Improved barriers to turbine engine fragments: interim report III. DOT/FAA/AR-99/8,III, Office of Aviation Research, Washington, DC, 20591
4. Kirkwood KM, Kirkwood JE, Lee YS, Egres RG Jr, Wagner NJ (2004) Text Res J 74(10):920
5. Billion HH, Robinson DJ (2001) Int J Impact Eng 25:411
6. Johnson GR, Beissel SR, Cunniff PM (1999) In: Proceedings of 18th international symposium on ballistics, vol 2. pp 962–969
7. Lim CT, Shim VPW, Ng YH (2003) Int J Impact Eng 28:13
8. Roylance D, Wilde A, Tocci G (1973) Text Res J 43:34
9. Shocky DA, Erlich DC, Simons JW (2002) Improved barriers to turbine engine fragments: interim report IV. 2002, DOT/FAA/AR-99/8,IV, Office of Aviation Research, Washington, DC, 20591
10. Duan Y, Keefe M, Bogetti TA, Powers B (2006) Int J Mech Sci 48:33
11. Zeng XS, Tan VBC, Shim VPW (2006) Int J Numer Methods Eng 66:1309
12. Pan N, Yoon MY (1993) Text Res J 63(11):629
13. Valizadeh M, Hosseini RSA, Salimi M, Sheikhzadeh M (2008) J Text Inst 99:37
14. Kalman DP, Merrill RL, Wagner NJ, Wetzel ED (2009) Appl Mater Interfaces 1(11):2602
15. Ma L, Bin Y, Sakai Y, Chen Q, Kurosu H, Matsuo M (2001) Macromolecules 34(14):4802
16. DuPont™ Vamac®, http://www2.dupont.com/Vamac/en_US/
17. Samant KR, Sauer BB, Minshon JC Fabrics with strain-responsive viscous liquid polymers. United States Patent Application Publication No.: US 2006/0286882 A1
18. Harkare A, Gillespie JW Jr (2004) J Thermoplast Compos Mater 17(5):387
19. Bastien LJ, Gillespie JW Jr (1991) Polym Eng Sci 31(24):1720